Microelectronics Journal 39 (2008) 660–663

Microelectronics Journal

www.elsevier.com/locate/mejo

Integrated InGaAsP MQW Mach–Zehnder modulator

D.A. May-Arrioja[a,*], P. LiKamWa[b], I. Shubin[c], P.K.L. Yu[c]

[a]*Photonics and Optical Physics Laboratory, Optics Department, INAOE, Apdo. Postal 51 y 216, Tonantzintla, Puebla 72000, Mexico*
[b]*CREOL & FPCE, The College of Optics and Photonics, University of Central Florida, Orlando, FL 32816, USA*
[c]*Department of Electrical and Computer Engineering, University of California, San Diego, CA 92093, USA*

Available online 23 August 2007

Abstract

We demonstrate the use of an area selective zinc in-diffusion process as a simple and efficient technique for the fabrication of integrated photonic devices. By controlling the profile of the diffusion front and the zinc depth the insertion losses of the devices can be minimized. Using this technique an integrated 1×2 Mach–Zehnder analog modulator was fabricated. Our experimental results demonstrate that the modulator exhibits excellent linearity for both TE and TM polarizations over a wavelength range of 40 nm. The measured on-chip losses in the order of 3 dB are obtained, which is significantly lower compared to the use of isolation trenches.

Keywords: Integrated optics; Electro-optic device; Modulator; Photonic integrated circuits; Multiple quantum wells; Semiconductor switches; Optical switch

1. Introduction

Optical modulators are essential components in advanced optical networks. For this reason, they have been fabricated on different material platforms. However, there is a remarkable interest on integrated technology because it provides highly robust products and costs are also decreased. In particular, InP-based compound semiconductors are very attractive because they are well suited for the monolithic integration of photonic and electronic devices. This is due mainly to two reasons. First, InP-based optical switches have the advantage of high-speed, low-power operation, and compact size [1–3] because of the enhanced refractive index change obtained by using the quantum-confined Stark effect (QCSE) in multiple quantum wells (MQW). They are also well suited for operation at 1.55 μm, the wavelength at which minimum dispersion and absorption occurs for silica fibers. Additionally, they are the perfect candidates for high-speed electronic devices because of the high-carrier mobility and saturation velocity of electrons. However, in order to achieve the level of integration required in next generation optical networks, very reliable and reproducible techniques for fabricating high-quality planar photonic and electronic integrated devices will be required. Among the different processes used for the fabrication of electronic devices, the diffusion of zinc plays an important role. Zinc is the most common p-type dopant, and has been widely used in the electronics industry. Zinc diffusion is also preferred to ion implantation because high zinc concentrations and deep junctions, which are required for some devices, can be easily achieved [4,5]. In this work, a zinc in-diffusion process in InP using a semi-sealed open-tube diffusion furnace was employed to fabricate highly localized p–n junctions on an n-type wafer. By controlling the background concentration of the wafer the diffusion profile can be easily controlled, and thus minimizing the free-carrier absorption. Using this process, an integrated InP Mach–Zehnder analog modulator was fabricated. Our experimental results demonstrate that the modulator exhibits excellent linearity for both TE and TM polarizations over a wavelength range of 40 nm. The technique proved to be very successful in defining isolated p–n junctions, demonstrating its potential in the fabrication of lightwave circuits.

*Corresponding author. Tel.: +52 222 247 2011x8115; fax: +52 222 247 2940.
E-mail address: dmay@inaoep.mx (D.A. May-Arrioja).

0026-2692/$ - see front matter © 2007 Elsevier Ltd. All rights reserved.
doi:10.1016/j.mejo.2007.07.053

2. Zinc in-diffusion in InP

It is generally accepted that the diffusion mechanism of zinc in InP is governed by an interstitial–substitutional mechanism. This diffusion mechanism can be modeled by a one-dimensional diffusion equation with a concentration-dependent diffusion coefficient [6],

$$\frac{\partial C_s}{\partial t} = \frac{\partial}{\partial x}\left(D_{\text{eff}}\frac{\partial C_s}{\partial x}\right), \tag{1}$$

where C_s is the concentration of substitutional ions, and D_{eff} is the concentration-dependent diffusion coefficient given by $D_{\text{eff}} = D_0 C_s^n$, with D_0 being a diffusion constant. The equation can be solved for the case of constant surface concentration and a semi-infinite medium. Shown in Fig. 1 (inset) are the normalized diffusion profiles obtained from Eq. (1) for the cases of $n = 0$, 1, 2, and 3 (depth axis normalized to $n = 1$). The case of $n = 0$ corresponds to the typical complementary error function solution that is obtained for a constant diffusion coefficient. The main feature in the inset of Fig. 1 is that a sharper diffusion front is obtained as the order n is increased, which is ideal to minimize free-carrier absorption. Interestingly, the order n of the concentration-dependent diffusion coefficient is highly depend on the initial background donor concentration of the wafer. Highly n-type-doped InP wafers ($\sim 1\times10^{18}\,\text{cm}^{-3}$) typically exhibit a cubic dependence of the diffusion constant ($n = 3$), whereas undoped wafers ($\sim 1\times10^{15}\,\text{cm}^{-3}$) exhibit a linear dependence ($n = 1$) [7]. Intermediate doping concentration on the order of 1×10^{17} should reveal a quadratic dependence ($n = 2$) [6]. This allows a simple way of controlling the required diffusion front.

The wafer structure used in this work consisted of an n–i–n structure similar to the one used in Ref. [8]. The n-doped InP layers were grown with a doping concentration of $2\times10^{17}\,\text{cm}^{-3}$, which should provide an $n = 2$ dependence of the diffusion profile. The zinc in-diffusion process was performed using a semi-sealed open-tube technique, which is also explained in Ref. [8]. The experimental zinc diffusion profile at 500 °C for a duration of 30 min is shown in Fig. 1. A zinc depth of 0.8 μm with a sharp diffusion front was obtained for this diffusion time. Also shown in Fig. 1 is the theoretical diffusion profile for $n = 2$, which fits very well in the experimental profile. We should highlight that the zinc depth can be easily modified by simply changing the diffusion time, while keeping the remaining parameters constant.

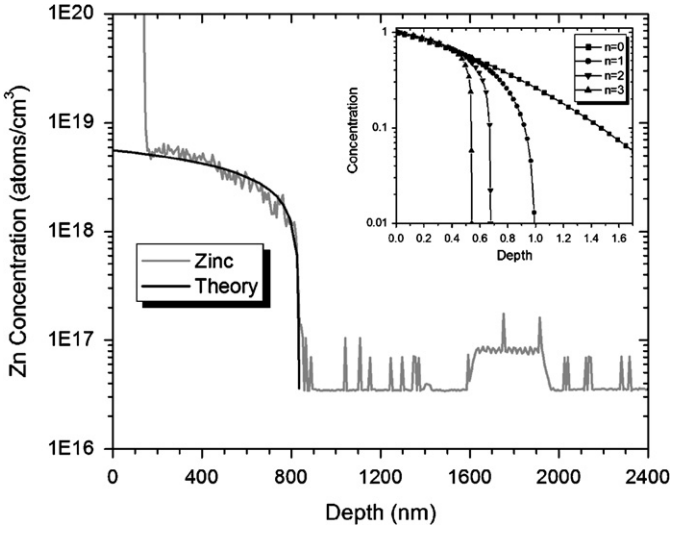

Fig. 1. Experimental zinc diffusion profile and theoretical fitting ($n = 2$) for 30 min. Diffusion at 500 °C (inset: zinc diffusion profiles for different powers of the diffusion coefficient).

3. 1 × 2 Mach–Zehnder structure

A schematic of the fabricated Mach–Zehnder modulator is shown in Fig. 2. It consists of a 500-μm-long input waveguide that launches the light into a 160 μm long symmetric 1×2 multimode interference (MMI) splitter. The control arms of the interferometer are 800 μm long and separated by 3 μm. After the control arms, a 484 μm long 3-dB MMI coupler is used to recombine the signals. Two 500-μm-long waveguides are used as the output of the device. All the waveguides are 3 μm wide and the total length of the device is 2.44 mm. The principle of operation is as follows: the input light is divided by the 1×2 MMI into two optical beams. The two light beams follow different paths to the separate arms of the 3-dB MMI coupler. With no electric field applied to the control arms, the optical fields that enter the arms of the MMI coupler are in phase. Therefore, the output ports of the device shares equal power. When an electric field is applied to one control arm of the interferometer, and a $\pi/2$ relative phase change is introduced, the light is switched completely to the output that is connected to that arm. Depending on which arm we apply the field, we can switch the light from one output to the other. In general two requirements need to be met in order for the switch to work properly. We need to be able to induce a $\pi/2$ phase shift and also fabricate a 3-dB coupler. The first one can be easily achieved because the QCSE allows us to induce large index changes. As for the 3-dB coupler, the use of an MMI structure significantly reduces the effort to achieve a perfect 3-dB coupler.

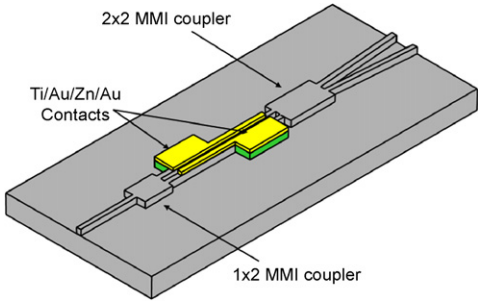

Fig. 2. Schematic of the Mach–Zehnder modulator.

4. Device fabrication and experimental results

Fabrication of the integrated device was initiated by the deposition of a 200 nm thick Si_3N_4 film using plasma enhanced chemical vapor deposition (PECVD). Conventional photolithography, followed by a CF_4 plasma etching was used to define the two 700 μm long diffusion windows. The Si_3N_4 film is used as a mask for the Zn diffusion process. Zinc was then diffused into the sample using the process described in Ref. [8]. The Mach–Zehnder modulator was then patterned by photolithography, followed by dry etching using an H_2/CH_4 plasma. The sample was then planarized using benzocyclobutene (BCB) planarization film. Ti/Zn/Au p-type contacts were patterned on top of the zinc-diffused areas. Finally, after the wafer was lapped to a thickness of 150 μm and polished to a mirror finish, the sample was cleaved and mounted on a copper header in preparation for device testing. A photograph of the fabricated device is shown in Fig. 3.

The device characteristics were investigated by coupling light from a tunable semiconductor laser into the input waveguide using a 40× microscope objective lens. The light from the output waveguides of the switch was collected using a 20× microscope objective lens. A beam splitter was used to split the light so as to allow monitoring of the output facet using an infrared Vidicon camera and measuring the output powers in the two output ports of the switch using an InGaAs photo-detector. The input beam was modulated by a mechanical chopper and the detected output beam intensity was measured using a lock-in amplifier. The bias voltage was applied to one arm of the interferometer while the other arm was grounded. The output power from the left output port was recorded as a function of the applied voltage at a laser wavelength of 1.55 μm, and is shown in Fig. 4. Although the extinction ratio is only about −12 dB for TE polarization, the key parameter for analog modulation is linearity. As can be observed the device response exhibits excellent linearity. Excellent linearity is also obtained for TM polarization as shown in the inset of Fig. 4. In this case a slight higher voltage is required, which is typical for lattice matched MQW. Similar voltage requirements for both polarizations could be obtained by improving the waveguide structure and using a strained MQW wafer structure that compensate for the MQW polarization dependence [9]. The device linearity was maintained over a wavelength range of 40 nm.

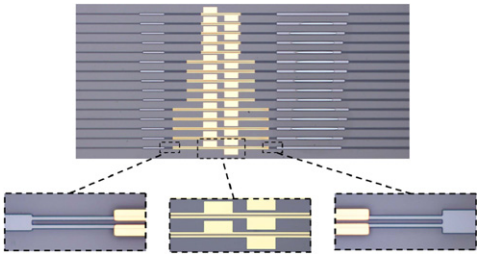

Fig. 3. Picture of fabricated Mach–Zehnder modulator.

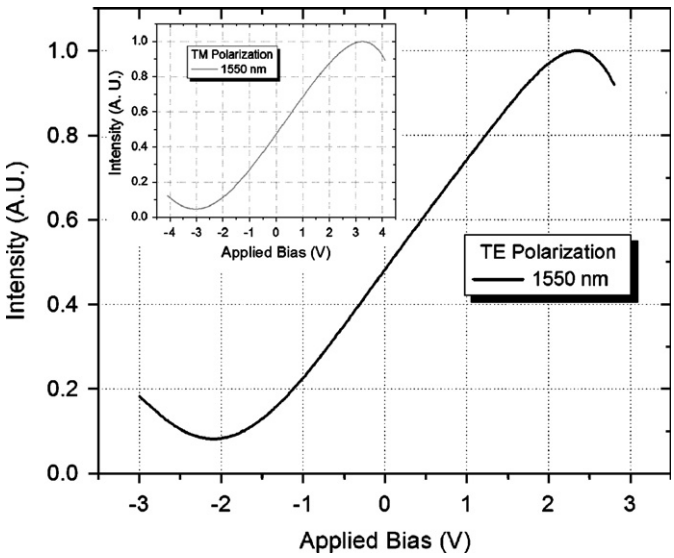

Fig. 4. Experimental analog modulation for TE and TM (inset) polarizations.

On-chip losses of only 3 dB were obtained in our device, which is significantly lower when compared to ~3 dB per isolation trench. This is a result of controlling the zinc profile and depth. We should also emphasize that due to the back-to-back diode structure formed by the two p–n junctions, the modulator could be fully controlled applying an analog signal to the contacts. It should also be noticed that by simple switching the electrical probes, the response of the device is also inverted.

5. Conclusions

An area-selective zinc-in diffusion technique was successfully characterized for the development of photonic integrated circuits. By controlling the wafer background concentration, we were able to control the diffusion front, and thus minimize the free-carrier losses resulting from the diffusion process. The method is simple yet highly controllable and reproducible. As a prove of concept an integrated 1 × 2 Mach–Zehnder analog modulator was fabricated. Our experimental results demonstrate that the modulator exhibits excellent linearity for both TE and TM polarizations over a wavelength range of 40 nm. The measured on-chip losses in the order of 3 dB are obtained, which is significantly lower compared to the use of isolation trenches.

References

[1] O. Leclerc, P. Brindel, D. Rouvillain, E. Pincemin, B. Dany, E. Desurvire, C. Duchet, E. Boucherez, S. Bouchoule, 40 Gbit/s polarization-insensitive and wavelength-independent InP Mach–Zehnder modulator for all-optical regeneration, Electron. Lett. 35 (1999) 730–731.

[2] N. Agrawal, C.M. Weinert, H.-J. Ehrke, G.G. Mekonnen, D. Franke, C. Bornholdt, R. Langenhorst, Fast 2 × 2 Mach–Zehnder optical

space switches using InGaAsP–InP multiquantum-well structures, IEEE Photon. Technol. Lett. 7 (1995) 644–645.
[3] A. Sneh, J.E. Zucker, B.I. Miller, Compact, low-crosstalk, and low-propagation-loss quantum-well Y-branch switches, IEEE Photon. Technol. Lett. 8 (1996) 1644–1646.
[4] C. Blaauw, F.R. Shepherd, D. Eger, Secondary ion mass spectrometry and electrical characterization of Zn diffusion in n-type InP, J. Appl. Phys. 66 (1989) 605–610.
[5] I. Yun, K.-S. Hyun, Zinc diffusion process investigation of InP-based test structures for high-speed avalanche photodiode fabrication, Microelectron. J. 31 (2000) 635–639.
[6] G.J. Van Gurp, P.R. Boudewijn, M.N.C. Kempeners, D.L.A. Tjaden, Zinc diffusion in n-type indium phosphide, J. Appl. Phys. 61 (1987) 1846–1855.
[7] H.B. Serreze, H.S. Marek, Zn diffusion in InP: effect of substrate dopant concentration, Appl. Phys. Lett. 49 (1986) 210–211.
[8] D.A. May-Arrioja, N. Bickel, P. LiKamWa, Optical beam steering using InGaAsP multiple quantum wells, IEEE Photon. Technol. Lett. 17 (2005) 333–335.
[9] J.E. Zucker, K.L. Jones, T.H. Chiu, B. Tell, K. Brown-Goebeler, Strained quantum wells for polarization-independent electrooptic waveguide switches, J. Lightwave Technol. 10 (1992) 1926–1930.